Transport properties of pure and doped *M*NiSn (*M*=Zr, Hf)

C. Uher
Department of Physics, University of Michigan, Ann Arbor, Michigan 48109

J. Yang
Department of Physics, University of Michigan, Ann Arbor, Michigan 48109
and Physics & Physical Chemistry Department, General Motors Research and Development Center, Warren, Michigan 48090-9055

S. Hu
Department of Physics, University of Michigan, Ann Arbor, Michigan 48109

D. T. Morelli and G. P. Meisner
Physics & Physical Chemistry Department, General Motors Research and Development Center, Warren, Michigan 48090-9055
(Received 16 October 1998)

We have studied the transport properties in a family of pure and doped intermetallics of the form *M*NiSi (*M*=Zr, Hf), the structures known as the half-Heusler alloys. We have shown that the transport is very sensitive to structural arrangements of the constituent atoms, and this can be manipulated by annealing, isostructural alloying, and doping. The unusual transport properties are viewed in the context of a semimetal-semiconductor transition that in pure alloys sets in near 150 K. Doping with indium can shift the transition upward towards 200 K. The high-temperature transport is dominated by the presence of heavy electrons that are responsible for surprisingly large values of thermopower. Minute amount of antimony (*n*-type doping) have a spectacular influence on the nature of transport and drive the electrical resistivity and Hall effect to be metal-like at all temperatures. Sb-doped alloys display very high thermoelectric power factors, but the thermal conductivity is still too high to make the material a prospective thermoelectric. [S0163-1829(99)07013-7]

I. INTRODUCTION

Complex intermetallic systems have been of considerable interest in recent years for their interesting magnetic behavior and unconventional transport properties. One of the most intriguing intermetallics are the ternary compounds of the general formula *M*NiSn (*M*=Zr, Hf, Ti), frequently referred to as the half-Heusler alloys. These compounds possess MgAgAs structure[1] and are closely related to the full Heusler alloys $M\mathrm{Ni}_2\mathrm{Sn}$ that are built up of four interpenetrating fcc sublattices mutually shifted along the body diagonal by a $\frac{1}{4}$ distance. While the full Heusler alloys are metals, removal of the Ni atoms on one of the two Ni sublattices and replacing them by an ordered lattice of vacancies leads to the formation of the paramagnetic half-Heusler intermetallics with a small gap in the density of states and a substantially semiconducting character.

Previous transport studies[2–4] established the magnitude of the gap as 0.1–0.2 eV and suggested a very high value of the thermopower that arises as a consequence of the narrow band with heavy carrier mass. These features drew the attention of researchers searching for systems with promising thermoelectric properties.[5,6]

We have decided to explore the transport properties of the half-Heusler intermetallics in detail and investigate what kind of structural modifications might lead to optimization of the transport parameters from the perspective of useful thermoelectric materials. Specifically, we were interested in establishing the effectiveness of isoelectronic alloying on the *M* sublattice and in finding whether one can alter the carrier density by doping on the Sn sublattice. In this paper we report on our measurements.

II. MATERIALS AND EXPERIMENTAL TECHNIQUE

Samples for this study were made from high-purity materials (Zr and Hf of 99.99% purity, other elements 99.999% pure) by arc melting under argon. We made stoichiometric compositions of *M*NiSn (*M*=Zr, Hf), isoelectronic alloys of the form $\mathrm{Zr}_{0.5}\mathrm{Hf}_{0.5}\mathrm{NiSn}$, *n*-type alloys $\mathrm{Zr}_{0.5}\mathrm{Hf}_{0.5}\mathrm{NiSb}_x\mathrm{Sn}_{1-x}$, and *p*-type-doped $\mathrm{ZrNiIn}_x\mathrm{Sn}_{1-x}$ and $\mathrm{HfNiIn}_x\mathrm{Sn}_{1-x}$. In all cases, the alloyed sample was arc remelted at least 3 times to ensure its homogeneity. Samples were cut using a diamond wheel and had dimensions of $2\times3\times8$ mm^3. The pure ZrNiSn and HfNiSn samples as well as their isoelectronic alloy $\mathrm{Zr}_{0.5}\mathrm{Hf}_{0.5}\mathrm{NiSn}$ were measured as prepared (without annealing) and also following 2 day and 1-week anneals at 800 °C. All other structures were measured following a standard 1-week anneal at 800 °C. X-ray analysis revealed a single-phase structure for all alloys.

Measurements were made over the temperature range of 2–300 K in a cryostat equipped with a radiation shield. Thermal transport parameters (thermopower and thermal conductivity) were determined using a longitudinal steady-state technique. The Hall effect and electrical resistivity were measured using a Linear Research ac bridge with 16 Hz excitation in a magnet cryostat capable of fields up to 5 T. Samples used in the study and some of their key parameters are given in Table I.

TABLE I. Room temperature values of the transport parameters. Samples without an asterisk were subjected to no annealing treatment. Samples with a single asterisk were annealed for 2 days; those with two asterisks were annealed for a 1-week period.

Sample	ρ ($\mu\Omega$ m)	κ (W/m K)	S (μV/K)	n (10^{20} cm^{-3})	μ_H (cm^2/V s)
ZrNiSn	51	5.9	−167	1.84	6.7
ZrNiSn*	113	8.6	−171	0.90	6.1
ZrNiSn**	201	17.2	−210	0.21	14.8
$Zr_{0.5}Hf_{0.5}NiSn$	105	4.6	−136	1.00	6.0
$ZR_{0.5}Hf_{0.5}NiSn$*	161	4.3	−142	0.39	10.0
$Zr_{0.5}Hf_{0.5}NiSn$**	289	5.3	−203	0.24	9.01
$ZrNiSn_{0.995}In_{0.005}$**	250	8.0	−105	1.57	1.59
$ZrNiSn_{0.99}In_{0.01}$**	418	8.1	−99	0.21	7.3
$HfNiSn_{0.995}In_{0.005}$**	717	9.8	−141	0.08	10.9
$HfNiSn_{0.99}In_{0.01}$**	540	7.4	−104	0.31	3.73
$Zr_{0.5}Hf_{0.5}NiSn_{0.995}Sb_{0.005}$**	16	6.0	−149	1.30	30.0
$Zr_{0.5}Hf_{0.5}NiSn_{0.99}Sb_{0.01}$**	8	6.6	−196	2.10	37.2

III. RESULTS AND DISCUSSION

A. Undoped ZrNiSn, HfNiSn, and $Zr_{0.5}Hf_{0.5}NiSn$

The *M*NiSn structure, on account of its vacancy sublattice, is an open structure, and any kind of disorder on the vacancy sublattice is likely to have a profound effect on the band gap and consequently on the transport behavior. Furthermore, the similar size of the Zr (0.16 nm) and Sn (0.158 nm) atoms may lead to a significant degree of mutual substitution and hence disorder on both the Zr and Sn sublattices. The size of Hf atoms is not as near the size of Sn atoms, and the intermixing should be of lesser concern. Since intermixing between the sublattices depends on the heat treatment, we have made a series of measurements monitoring transport properties as a function of annealing conditions. We start with the behavior of thermal conductivity as this quantity is extremely sensitive to structural disorder and is thus a very good indicator of the evolving perfection of the crystal lattice. Figure 1 shows the temperature dependence of the total thermal conductivity for ZrNiSn [Fig. 1(a)]. HfNiSn [Fig. 1(b)], and $Zr_{0.5}Hf_{0.5}NiSn$ [Fig. 1(c)] subjected to different annealing periods. For all structures we observe dramatic changes in the thermal conductivity with prolonged annealing. The pure intermetallics ZrNiSn and HfNiSn show greatly enhanced thermal conductivity upon annealing. This is especially notable at low temperatures where, after a week of annealing, the peak in $\kappa(T)$ grows by a factor of 3 in comparison to the samples subjected to no annealing. This clearly reflects an improvement in the structural quality of the annealed material. A very different picture emerges upon annealing an isoelectronic $Zr_{0.5}Hf_{0.5}NiSn$ alloy. Apart from the fact that the overall thermal conductivity is suppressed due to the mass-defect scattering between Zr ($M_{ZR}=91$) and Hf ($M_{Hf}=179$), we note an opposite trend upon annealing—the thermal conductivity decreases. This implies that the as-prepared isoelectronic alloy does not have the *M* sublattice initially fully randomized and it takes a heat treatment to assure that Zr and Hf atoms are completely mixed. We also note that essentially the entire thermal conductivity is due to lattice phonons; the electronic component of thermal conductivity is at the level of no more than 1%. Furthermore, it is interesting to point out that although HfNiSn has a higher thermal conductivity than ZrNiSn for all comparable stages of annealing, the percentage increase in $\kappa(T)$ after 1 week of annealing is similar for the two compounds. We thus see no evidence of significantly greater intermixing between Zr and Sn (in comparison to Hf and Sn) with prolonged annealing.

Figure 2 shows the behavior of electrical resistivity. Three striking features are notable: very large resistivity, strong dependence on annealing, and an unusual temperature dependence. Samples subjected to no heat treatment have similar resistivities at 4 K in the range between 150 and 200

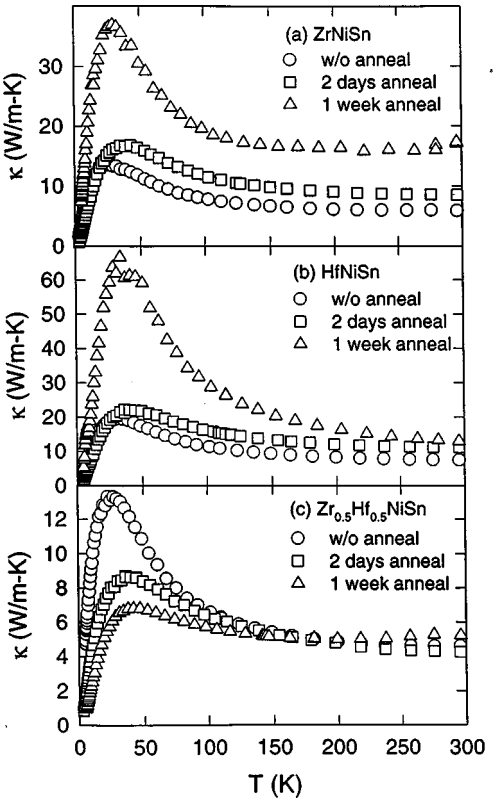

FIG. 1. Thermal conductivity as a function of temperature for different annealing periods: (a) ZrNiSn, (b) HfNiSn, (c) $Zr_{0.5}Hf_{0.5}NiSn$.

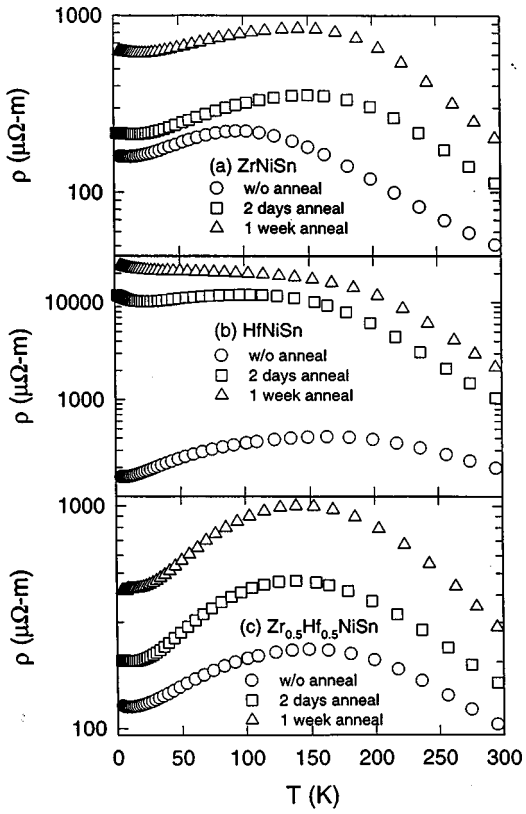

FIG. 2. Temperature dependence of electrical resistivity for different annealing conditions: (a) ZrNiSn, (b) HfNiSn, and (c) $Zr_{0.5}Hf_{0.5}NiSn$.

$\mu\Omega$ m. These are very high resistivities for systems that display metal-like character (positive $d\rho/dT$) for temperatures below 100–150 K, and the carrier mean free path must undoubtedly be very short. Remarkably, $\rho(4\ \mathrm{K})$ increases rapidly upon annealing, and after 1 week at 800 °C it becomes a factor of 4 larger in ZrNiSn and $Zr_{0.5}Hf_{0.5}NiSn$, and in HfNiSn it shoots up by two orders of magnitude. Although the metal-like character of $\rho(T)$ at low temperatures is somewhat less pronounced (below 10–15 K one observes a turnaround and increasing resistivity with decreasing temperature), the positive temperature coefficient of resistivity is still clearly preserved in ZrNiSn and $Zr_{0.5}Hf_{0.5}NiSn$. In contrast, HfNiSn after 1 week of heat treatment never attains any kind of metallic character. It was argued by Aliev *et al.*[2] that due to the similar sizes of Zr and Sn atoms there is a considerable degree of intermixing on the two respective sublattices which may reach values as high as 30%. Prolonged annealing would presumably promote such a process. Because far greater changes upon annealing are seen in HfNiSn than in either ZrNiSn or $Zr_{0.5}Hf_{0.5}NiSn$, and yet Hf and Sn atoms have more incompatible sizes than Zr and Sn, the intermixing between the *M* and Sn sublattices may not be the dominant effect behind the rising resistivity following heat treatment. As we have already noted, thermal conductivity data do not support a notion of strong intermixing between Zr and Sn or Hf and Sn promoted by annealing. In fact, we are left with a puzzling situation that, from the perspective of phonon transport, annealing of ZrNiSn and HfNiSn is very beneficial, while this same heat treatment has a very deleterious effect on the transport of charge carriers.

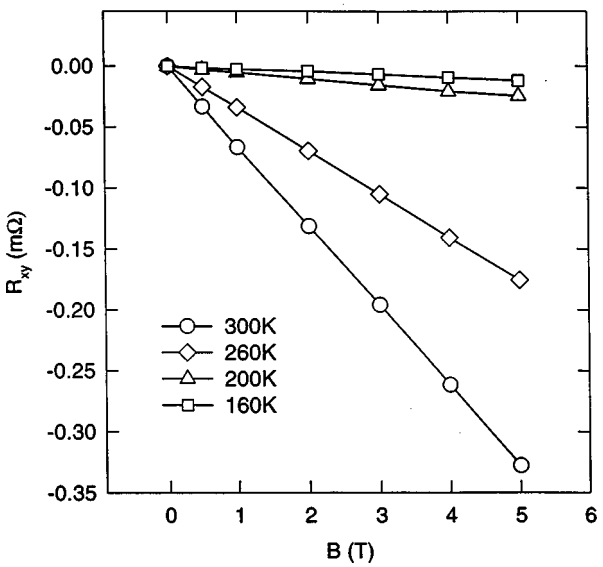

FIG. 3. Hall resistance vs magnetic field measured on 1-week-annealed ZrNiSn at several different temperatures. Note a linear dependence on the field and a rapidly diminishing slope of the lines as the temperature decreases.

An additional peculiar feature of carrier transport is its temperature dependence. In the absence of magnetic phase transitions (the structures are Pauli paramagnets), it is very unusual to observe metal-like transport at low temperatures turning into a semiconducting behavior at ambient temperatures. To shed light on the situation, we made measurements of the Hall effect over a broad temperature range from 4 to 300 K. The data for 1-week-annealed ZrNiSn, plotted in the form of the Hall resistance versus magnetic field at several temperatures, are shown in Fig. 3. Similar plots have been collected for other undoped structures and various annealing treatments. The essential feature of the data is a linear field dependence of the Hall resistance and its rapidly decreasing slope with the falling temperature. Straight lines imply a single-carrier-dominated transport, and the inverse of the slope is proportional to the carrier density. It is clear then that, as the temperature decreases, the diminishing slope signals a rapidly increasing population of free carriers (electrons). In fact, below about 150 K, the Hall signal becomes very small, the slope is essentially zero and we cannot resolve further changes even with our sensitive ac technique. The carrier densities extracted from the data are plotted in Fig. 4. We note a decrease in the carrier density with annealing in both ZrNiSn and $Zr_{0.5}Hf_{0.5}NiSn$ (measurements were not made on HfNiSn), which correlates with the increasing resistivity depicted in Fig. 2. More important, we observe a very dramatic increase in the carrier density as the temperature decreases. This suggests that the unusual temperature dependence of resistivity in Fig. 2 is not the result of some exotic scattering mechanism, but, rather, it arises as a consequence of crossing over from the semiconducting to metallic or semimetallic regime of conduction as a result of band structure changes. Perfectly ordered half-Heusler alloys are small-gap semiconductors [theoretical indirect gap of about 0.5 eV (Ref. 7)], but any kind of disorder may shrink or even close the gap. For instance, the authors of Ref. 7 estimate that 15% intermixing between Zr and Sn is sufficient to close

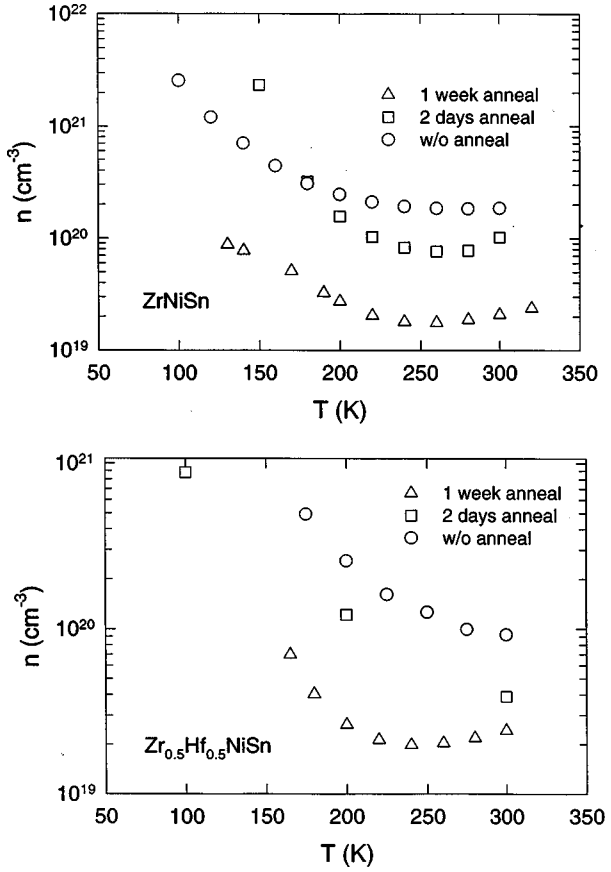

FIG. 4. Carrier densities as a function of temperature for ZrNiSn and $Zr_{0.5}Hf_{0.5}NiSn$ obtained from the sets of data such as illustrated in Fig. 3.

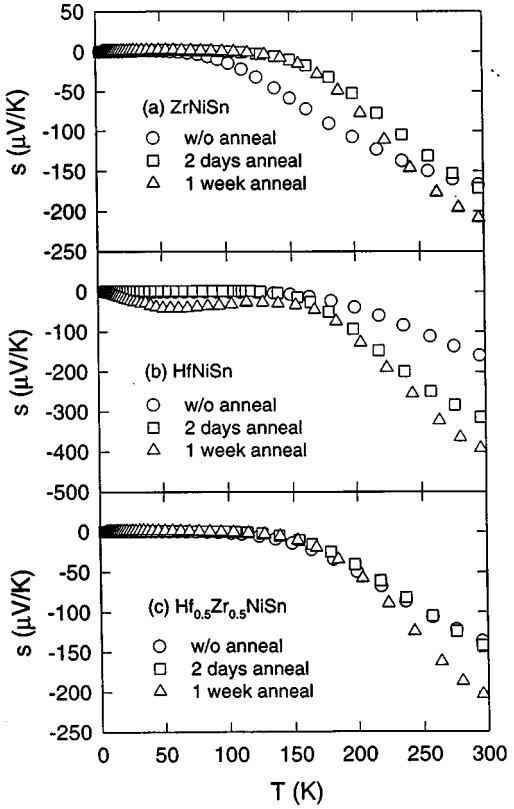

FIG. 5. Thermopower as a function of temperature for different annealing conditions: (a) ZrNiSn, (b) HfNiSn, and (c) $Zr_{0.5}Hf_{0.5}NiSn$.

the gap and form a semimetal. If, in addition, the gap is a strong function of temperature, it is then possible to picture a semimetal-semiconductor transition occurring near 150 K. The carrier density depends on the degree of band overlap that is controlled by the disorder, and this, in turn, is influenced by annealing. We shall see further evidence of this band-structure-dominant transport later when we discuss the influence of doping. Before we do so, we present the thermopower data on the undoped structures that we believe strongly support the idea of a semimetal-semiconductor transition. These are shown in Fig. 5.

In all three panels of Fig. 5, we see a distinct trend: a nearly constant thermopower with a very small positive slope extending to temperatures of 100–150 K, followed by a rapidly rising negative thermopower that reaches values in excess of several hundred μV/K near 300 K. The break from a small and approximately linear thermopower at low temperatures correlates very well with the position of the peak in resistivity as shown in Fig. 2. The thermopower thus faithfully reflects the predominant mode of transport—metallic (semimetallic) character at low temperatures switching over to a semiconducting behavior at higher temperatures. Combining results of the Hall effect and thermopower, we can estimate[8] the effective mass of electrons responsible for the large negative thermopower with the aid of Eqs. (1) and (2):

$$S=-\frac{k_B}{e}\left[\frac{2F_1(\eta)}{F_0(\eta)}-\eta\right], \tag{1}$$

$$n=\frac{4}{\sqrt{\pi}}\left[\frac{2\pi m^* k_B T}{h^2}\right]^{3/2} F_{1/2}(\eta), \tag{2}$$

where $\eta=E_F/k_BT$ and F_x is a Fermi integral of order x. The resulting effective masses are about $(2-3)m_e$ for ZrNiSn and of the order of $1m_e$ for $Zr_{0.5}Hf_{0.5}NiSn$. It is this rather heavy electron mass that leads to the large negative thermopowers observed at higher temperatures. On the other hand, a small, positive, and nearly linear thermopower at low temperatures suggests that the material is in a semimetallic domain of conduction. High carrier density and a negligibly small Hall effect (i.e., a near perfect compensation) below 150 K corroborate this picture. Effective masses of comparable magnitude were reported by Aliev *et al.*[9] based on a study of the electronic specific heat.

In the following we turn our attention to doping on the Sn sublattice. We were interested not only in optimizing thermoelectric properties of the *M*NiSn compounds, but primarily to glean what happens to the band structure and what further input such investigations provide to affirm the picture of a semimetal-semiconductor transition.

B. Indium-doped ZrNiSn and HfNiSn

The group-III element indium introduces a single hole when it replaces tin, the group-IV element. By doping with In we hoped to compensate for the dominant influence of the heavy electron band. With doping levels up to 5 at. % In, we succeeded only partially in altering the transport behavior. Figure 6 shows the temperature-dependent resistivity. While

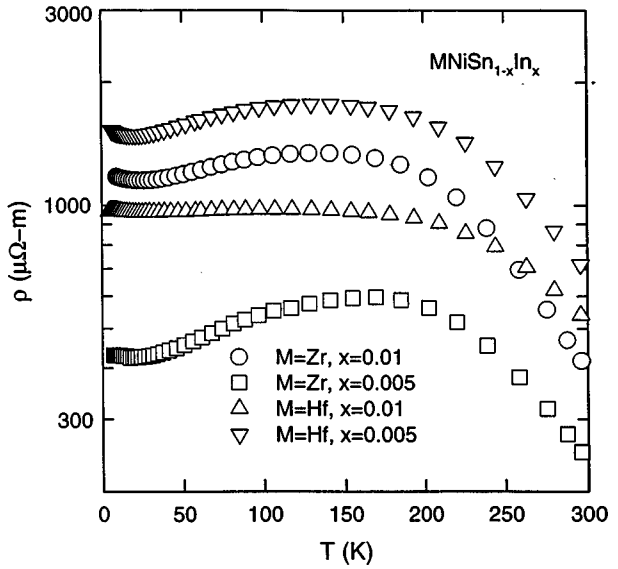

FIG. 6. Electrical resistivity of In-doped ZrNiSn and In-doped HfNiSn both annealed for 1 week.

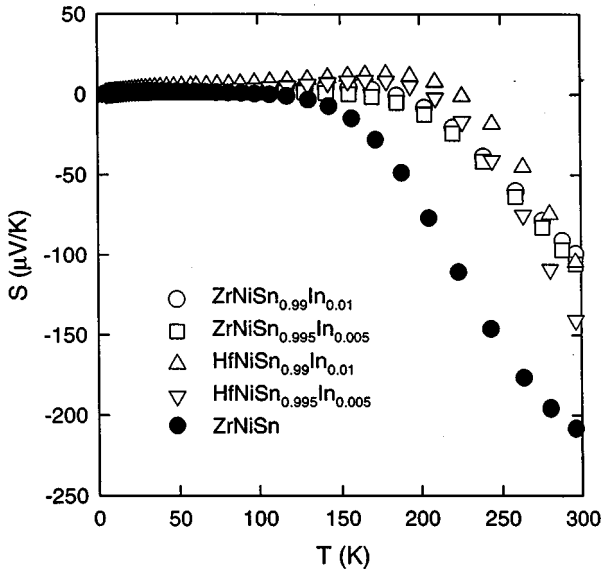

FIG. 8. Temperature dependence of thermopower for In-doped ZrNiSn. For comparison, we also show the data for pure ZrNiSn with the same 1-week annealing treatment.

the character of the transport—a changeover from a metal-like dependence at low temperatures to a semiconducting behavior at higher temperatures—is similar in all samples, the magnitude of the resistivity does not show a particular trend. We observe a contrasting behavior between Zr- and Hf-based structures. In the former case the resistivity appears to increase in the more heavily doped structures, while in the latter case the opposite is seen. In comparison to the undoped structures, the peak in the resistivity shifts towards 200 K rather than being near 150 K. This might suggest a greater degree of band overlap extending the semimetallic regime to higher temperatures. Strong supporting evidence for this viewpoint comes from the Hall effect measurements, Fig. 7. Large and linearly field-dependent Hall resistance rapidly diminishes with decreasing temperature, and near 200 K, essentially vanishes. Below 200 K we observe a small, positive Hall signal, but its field dependence is no longer linear. This would imply that a single-carrier, electron-dominated semiconducting regime of transport above 200 K gives way to a metal-like transport in which positively charged carriers play an important role. Nonlinearity in the field dependence of the Hall resistance supports the presence of more than one type of carrier—a scenario consistent with the semimetallic band structure.

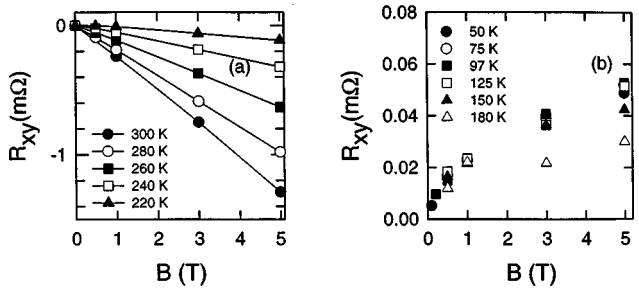

FIG. 7. Hall resistance as a function of magnetic field for In-doped HfNiSn. Panel (a) shows the data at higher temperatures; panel (b) shows low-temperature data. Note a change of sign between the high- and low-temperature data. The data for In-doped ZrNiSn show exactly the same trend.

The influence of positive carriers at low temperatures is also clearly seen in the behavior of the thermopower, Fig. 8. The *T*-dependent and positive thermopower for the In-doped alloys extends close to 200 K, some 50 K above the linear regime of the undoped *M*NiSn alloys. We include in Fig. 8 the data for ZrNiSn to visualize and appreciate the expanded regime of the positive thermopower in the In-doped structures. Above 200 K the thermopower turns rather abruptly negative and rapidly attains values on the order of -100 μV/K at 300 K. The gap has opened up, the structures become semiconducting, and the heavy electron band dominates the transport. Thus, with up to 5 at. % In, we have not been able to drastically change the nature of the conduction process; we only shifted the crossover regime by about 50 K towards higher temperatures.

C. Antimony-doped $Zr_{0.5}Hf_{0.5}NiSn$

The group-V element antimony serves the exactly opposite role than indium: it introduces an extra electron when substituted on the site of a tin atom. We have prepared two samples with a rather low level of antimony doping, 0.5 and 1 at. %. Since the isoelectronic alloy $Zr_{0.5}Hf_{0.5}NiSn$ shows promising reduction in its lattice thermal conductivity—the essential feature for any promising thermoelectric—we have chosen this matrix for our studies of *n*-type doping. In view of the comparable carrier transport behavior of pure *M*NiSn and of this isoelectronic alloy, we do not expect materially different results had pure ZrNiSn or HfNiSn been used as the starting alloy.

As Fig. 9 attests to, antimony doping has a spectacular effect on the transport behavior. The resistivity is nearly two orders of magnitude down, and its temperature dependence is entirely metallic. The carrier (electron) density obtained from the Hall effect is 2.1×10^{20} cm^{-3} for the 1 at. % Sb alloy and 1.2×10^{20} cm^{-3} for the 0.5 at. % Sb alloy, and both are essentially temperature independent. Thermopower behavior, Fig. 10, is also distinctly different—large negative

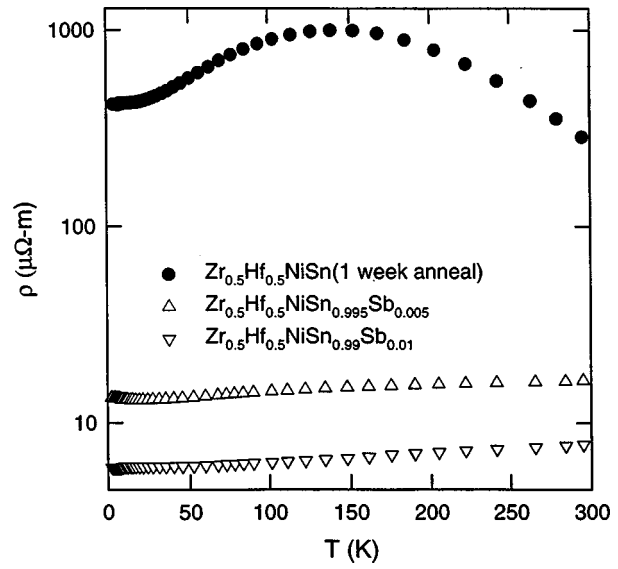

FIG. 9. Electrical resistivity for Sb-doped $Zr_{0.5}Hf_{0.5}NiSn$ alloys. For comparison, we also show the data for an undoped alloy of $Zr_{0.5}Hf_{0.5}NiSn$. Note a dramatically reduced magnitude of the resistivity and an entirely metal-like character of the temperature dependence.

values that increase approximately linearly with temperature are present already at low temperatures, and near the ambient temperature the thermopower reaches values of -150 to -200 μV/K. Such large magnitudes of thermopower, in conjunction with a significantly lower resistivity, are very appealing from the viewpoint of thermoelectricity. Indeed, the power factor $P=S^2/\rho$, where S is the thermopower and ρ the resistivity, reaches values of 23 and 28 μW/cm K^2) for $x_{Sb}=0.005$ and $x_{Sb}=0.01$, respectively. Such values are comparable to the best values obtained on state-of-the-art thermoelectric materials. Using again Eqs. (1) and (2), we estimate the effective masses for the two Sb-doped samples as $m^*=5.4$ ($x_{Sb}=0.005$) and $m^*=5.0$ ($x_{Sb}=0.01$). Heavy electrons are therefore at the core of the large thermopower, and the metallic character of transport suggests that the Fermi level intersects the heavy electron band.

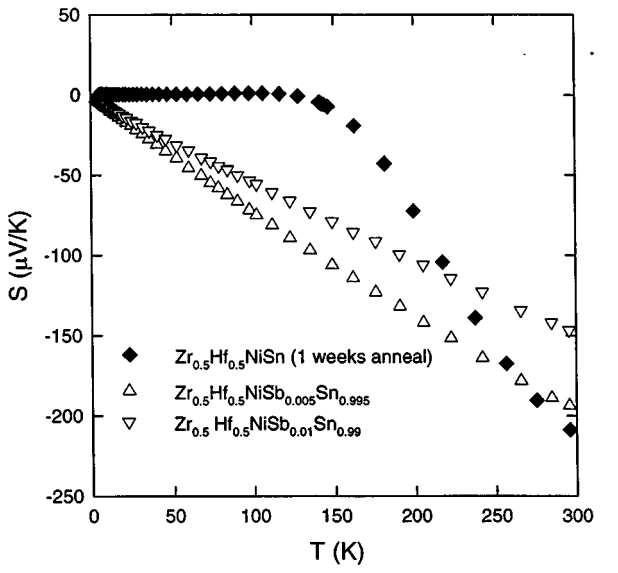

FIG. 10. Temperature dependence of thermopower of Sb-doped $Zr_{0.5}Hf_{0.5}NiSn$ alloys. For comparison, we also display the data for an undoped $Zr_{0.5}Hf_{0.5}NiSn$ alloy.

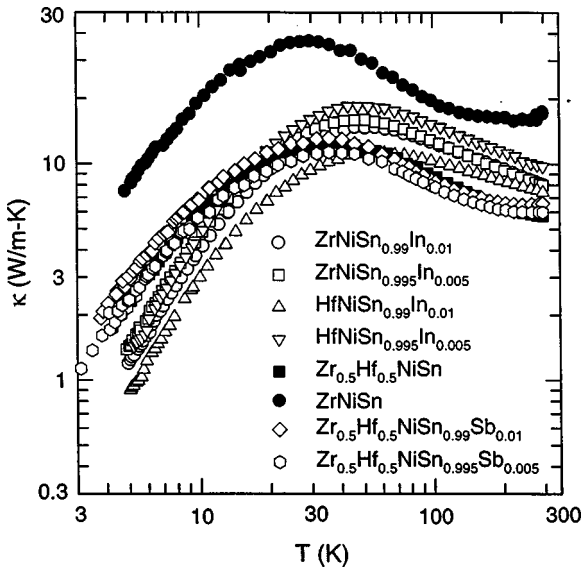

FIG. 11. Thermal conductivity of the doped half-Heusler alloys. For comparison, we also illustrate the data for 1-week-annealed ZrNiSn and $Zr_{0.5}Hf_{0.5}NiSn$.

In Fig. 11 we collect the data on the thermal conductivity of the doped structures. As a reference curve, we use the data for ZrNiSn annealed for the same 1-week period. It is easy to appreciate a reduction in thermal conductivity upon doping, especially the progressively disappearing peak in the In-doped alloys near 50 K. In the case of the two Sb-doped samples, we also see an additional influence of isoelectronic alloying that results in the lowest thermal conductivity values at ambient temperature. The lattice thermal conductivity of the Sb-doped samples is actually lower than the curves in Fig. 11 indicate by some 10–15%, the contribution we estimate as arising from the electronic thermal conductivity calculated using the Wiedemann-Franz law. On the other hand, in In-doped alloys the electronic contribution does not exceed 1% of the total thermal conductivity.

Lattice thermal conductivity values of 5–6 W/m K obtained on the Sb-doped alloys are still too high by a factor of 3 in comparison to state-of-the-art thermoelectrics such as Bi_2Te_3-based alloys. While the power factors of the Sb-doped isoelectronic alloys are very promising, more effort will be needed to lower the lattice thermal conductivity in order to make the material competitive in the thermoelectric area. It should be remembered, however, that so far we have explored structural modifications on only two of the three occupied sublattices of the half-Heusler alloys. There is still considerable phase space to be explored. Modifications (alloying and doping) on the Ni sublattice should be an interesting undertaking.

IV. CONCLUSIONS

In this paper we have discussed transport studies on pure and doped half-Heusler intermetallics of the general formula MNiSn (M=Zr, Hf). These materials possess a fascinating

structural arrangement with the constituent elements occupying separate fcc sublattices, and one sublattice consists of an ordered array of Ni vacancies. The physical properties of these alloys are very sensitive to a particular structural arrangement, and any kind of disorder has a strong influence on the transport behavior. Our extensive collection of transport data is consistent with a picture whereby the alloys at low temperatures are described as semimetals that crossover at higher temperatures into semiconductors with a small energy gap. The crossover temperature in the undoped structures is near 150 K, and it can be extended to higher temperatures upon *p*-type doping. Introducing even a minute amount of antimony (*n*-type doping) dramatically alters the nature of transport, and the alloys display entirely metallic characteristics, but with a surprisingly large magnitude of thermopower. The nature of the semimetal-semiconductor transition is undoubtedly connected with the state of disorder and strongly temperature-dependent band structure. The exact physical origin, however, must await studies such as photoelectron spectroscopy that can directly address issues concerning the band edges and the position of the Fermi level.

n-type doped isoelectronic alloys show remarkably high power factors that are in the class of the best thermoelectric materials. To make these alloys premier thermoelectrics requires further substantial reduction in their lattice thermal conductivity. Perhaps structural modifications on the Ni-occupied sublattice might be beneficial in this regard. Regardless, it appears that the optimal operational regime of the half-Heusler intermetallics as thermoelectrics would be at temperatures somewhat above 300 K. Appropriate transport studies should be extended into this temperature domain to assess properly the full potential of these alloys.

ACKNOWLEDGMENTS

This work was supported under ONR Grant No. 0014-96-10181 and in part by General Motors (J.Y.)

[1] W. Jeitschko, Metall. Trans. A **1**, 3159 (1970).

[2] F. G. Aliev, N. B. Brandt, V. V. Moshchalkov, V. V. Kozyrkov, R. V. Skolozdra, and A. I. Belogorokhov, Z. Phys. B **75**, 167 (1989).

[3] F. G. Aliev, Physica B **171**, 199 (1991).

[4] R. Kuentzler, R. Clad, G. Schmerber, and Y. Dossmann, J. Magn. Magn. Mater. **104-107**, 1976 (1992).

[5] B. A. Cook, J. L. Harringa, Z. S. Tan, and W. A. Jesser, *Proceedings of the 15th International Conference on Thermoelectrics, ICT96*, edited by T. Caillat *et al.* (IEEE, Piscataway, NJ, 1996), p. 122.

[6] H. Hohl, A. P. Ramirez, W. Kaefer, K. Fess, Ch. Thurner, Ch. Kloc, and E. Bucher, in *Thermoelectric Materials—New Directions and Approaches*, edited by T. Tritt *et al.*, MRS Symposia Proc. No. 478 (Materials Research Society, Pittsburgh, 1997), p. 109.

[7] S. Öğüt and K. M. Rabe, Phys. Rev. B **51**, 10 443 (1995).

[8] H. J. Goldsmid, *Applications of Thermoelectricity* (Methuen, London, 1960), pp. 32–33.

[9] F. G. Aliev, V. V. Kozyrkov, W. V. Moshehalkov, R. V. Scolozdra, and K. Durczewski, Z. Phys. B **80**, 353 (1990).